Electronic Supplementary Material (ESI) for Physical Chemistry Chemical Physics
This journal is © The Owner Societies 2013

Ultrafast branching in the excited state of coumarin and umbelliferone

Caroline M. Krauter[1], Jens Möhring[2], Tiago Buckup[2], Markus Pernpointner*[1], and Marcus Motzkus[2]

[1] *University Heidelberg, Theoretical Chemistry, Institute of Physical Chemistry, INF 229, 69120 Heidelberg, Germany. E-mail: Markus.Pernpointner@pci.uni-heidelberg.de*
[2] *University Heidelberg, Institute of Physical Chemistry, INF 229, 69120 Heidelberg, Germany.*

Contents

1 Additional Experimental Data

1.1 2D Transient Data

Figures SI.1 and SI.2 show 2D transient absorption maps for umbelliferone and coumarin. Selected transient absorption traces and spectra shown in Figures 2 and 3 were obtained from these data at the respective wavelengths and probe delays.

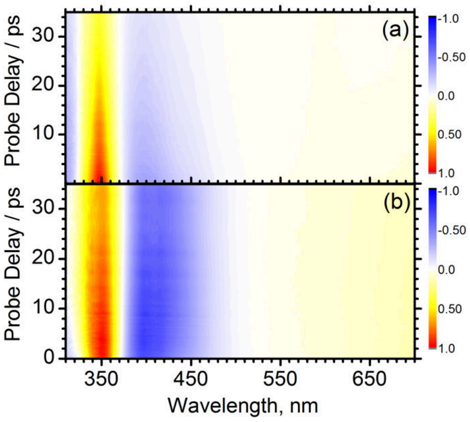

Fig. SI. 1: Transient absorption data of umbelliferone in (a) acetonitrile and in (b) methanol.

1.2 Expanded Target Analysis of Coumarin

The non-perfect agreement between the fitting model (Figure 12) and the data for coumarin in acetonitrile and methanol suggests the participation of an additional transient species. The deviation of kinetics model can be particularly observed at weak stimulated emission region of coumarin (Figure 14 (b) and (d)) . An expanded model, where an additional transient species is added between the components B and D can improve the fitting of the experimental data. Such an additional component may represent the evolution of the population in the excited state manifold of the nπ^* state. The application of this expanded model to, e.g., coumarin in methanol is shown in Figure SI.3 (compare red and black line in Figure SI.3). While the branching ratio obtained for the expanded does not change in comparison to the model of Figure 12, the additional component is populated with a similar time constant around 1-2 ps, but decays with 7-10 ps.

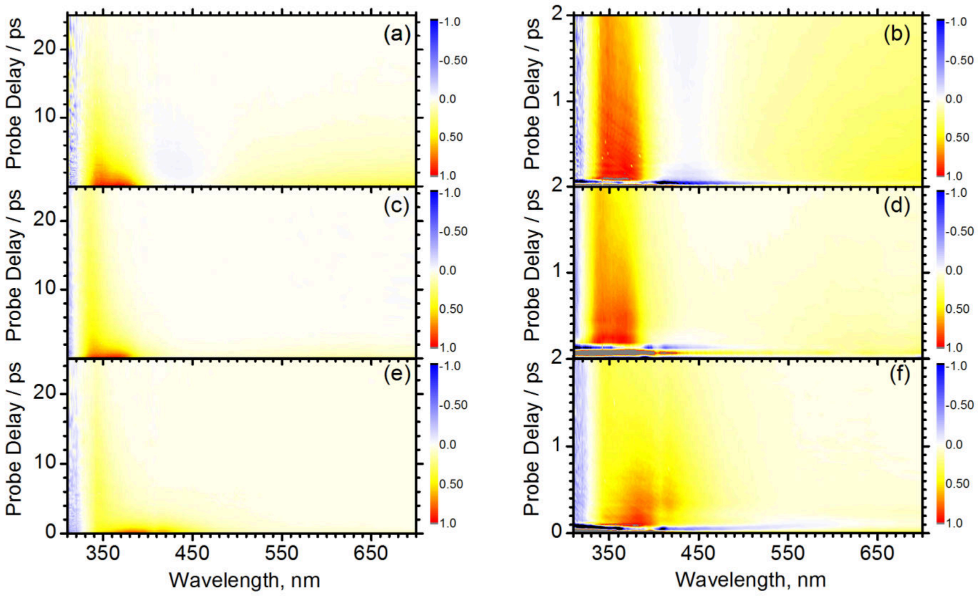

Fig. SI. 2: Transient absorption data of coumarin in (a)-(b) methanol, (c)-(d) acetonitrile and (e)-(f) cyclohexane. (b), (d) and (f) show in detail the first 2 ps of the transient dynamics of coumarin in each solvent.

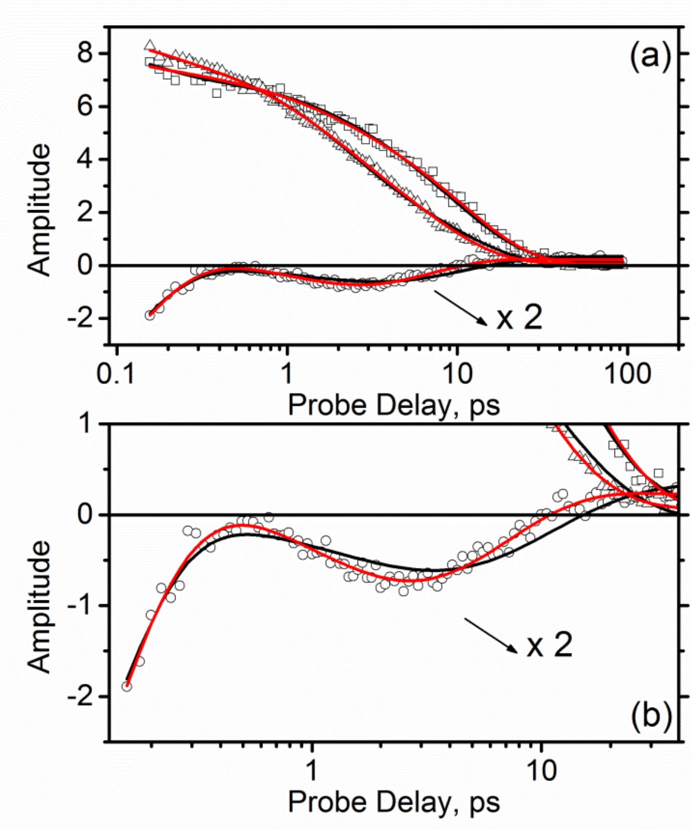

Fig. SI. 3: (a) Global target analysis results for coumarin in methanol using the model depicted in Figure 12 (black curve) and an expanded model using an additional contribution (red line). (b) The improvement of the fitting quality with the expanded model can be depicted at the SE region. See text for details on the expanded model. Data points are the same of Figure 14(b).

1.3 Global Target Analysis: Sequential Model

A sequential model involving 4 (A→B→C→D) and 5 (A→B→C→D→E) states was also investigated for both coumarins in all solvents. In all cases the sequential model did not fit well the transient molecular dynamics. Major deviations were observed e.g. for coumarin in methanol particularly in the SE band region (see Fig. SI.4), leading to a 10 % worse fitting in comparison to the model depicted at Fig. 12 in the main text. Time constants in this case were 1.9 ps, 10 ps and $>$ 500ps. The spectral shifting between component A and B can be relatively well fitted by the sequential model, but the transient signal at the SE band is completely missing in that model. Component C for coumarin in methanol has no amplitude. The fitting can be improved by 2 % for umbelliferone by adding one additional intermediate state to the sequential model (5 states in total), but it still is not able to fit the transient signal of coumarin in the SE band region.

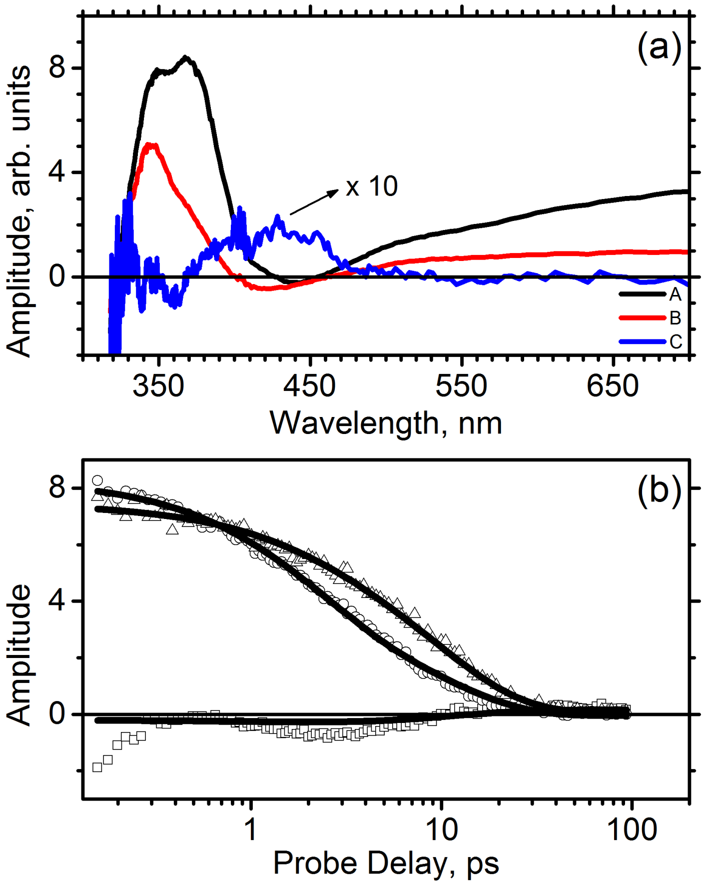

Fig. SI. 4: Global target analysis results for coumarin in methanol using a sequential model with 4 states (A→B→C→D). (a) Species associated spectra for each component. Note that the component C has almost no amplitude. (b) Transient absorption traces fitted with the model. Note the mismatch between fitting and experimental (open squares) at the maximum of the SE band.

1.4 Fluorescence spectrum of Umbelliferone

As has been discussed in section 5.5 of the paper, the anionic form of umbelliferone should play only a minor role in methanol solutions. However, to finally exclude any strong contribution, the fluorescence spectrum of umbelliferone in methanol was measured. The results are shown in Figure SI.5.

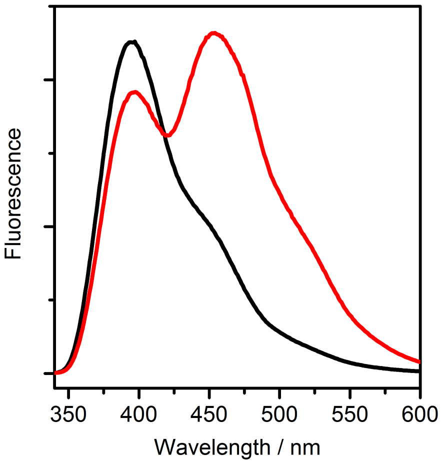

Fig. SI. 5: Fluorescence spectrum of umbelliferone in methanol (black curve) and a mixture of methanol and water (red curve, with about four volume percent water).

The fluorescence spectrum shows only one peak, however, with a small shoulder. The maximum of the peak lies at about 400 nm and the shoulder at about 450 nm. According to assignments made previously, e.g. [1], this correlates well with umbelliferone and a small amount of its anionic form. The presence of a small amount of anion is not surprising as the solvents used were not dried before the measurements and contained some traces of water which is known to influence the deprotonation of umbelliferone strongly [2]. Indeed, upon addition of more water, about four volume percent, the peak of the neutral form decreases while the peak of the anion increases strongly now exhibiting a higher intensity (compare Figure SI.5). This corresponds to our theoretical results, presented below, where a higher fluorescence quantum yield for the anionic form is obtained. Taking into account the higher fluorescence quantum yields, the relative amount of the anionic form is even smaller than indicated by the relative intensities.

Therefore, we conclude that despite some traces of water in our methanol solution, the anionic form plays only a minor role for the photochemical deactivation of umbelliferone in the solvents used. This is in accordance with our time-resolved measurements where no shoulder of the simulated emission (SE) band could be observed around 450 nm (compare Figures 2 and 13 in the paper). Both in methanol and in acetonitrile solution the SE bands were located at 400 nm and a shoulder around 450 nm was missing. Moreover, our model including only the two deactivation pathways discussed (no deprotonation) fits the experimental results almost perfectly. The same conclusion was obtained by, e.g., T. Moriya [1] and Bardez et al. [2].

2 Additional Theoretical Results

2.1 Structural Data

Table SI.1 contains a comparison of different basis sets used for ground state geometry optimizations of coumarin and a comparison with crystal structure data. Figure SI.6 shows the structures obtained by geometry optimizations in the first excited singlet $\pi\pi^*$ state of coumarin by TD-DFT (time-dependent density functional theory) methods applying two functionals which differ by their amount of exact Hartree-Fock exchange. For further discussion see Section 3.3.1 of the main paper. Finally, Figure SI.7 displays the minima on the gas phase PES of coumarin and umbelliferone in the 1^1A“ state.

(a) TD-B3LYP

(b) TD-BHLYP

Fig. SI. 6: $1^1A'$ minimum geometries of coumarin obtained with TD-B3LYP and TD-BHLYP. All bond lengths in Å. Basis set:aug-cc-pVTZ

Table SI. 1: Basis set dependence of bond lengths in coumarin. All values in Å. Numbering scheme according to paper. Method: MP2

Bond	x-ray[3]	cc-pVDZ	aug-cc-pVDZ	cc-pVTZ	aug-cc-pVTZ
O^1C^2	1.374	1.397	1.399	1.381	1.380
$C^2{=}O^{11}$	1.213	1.211	1.218	1.203	1.205
C^2C^3	1.454	1.468	1.466	1.450	1.450
$C^3{=}C^4$	1.347	1.361	1.364	1.344	1.345
C^4C^{10}	1.438	1.447	1.446	1.428	1.428
$C^{10}C^9$	1.397	1.412	1.412	1.394	1.395
C^9O^1	1.378	1.369	1.376	1.358	1.359
C^8C^9	1.394	1.404	1.404	1.387	1.386
C^7C^8	1.383	1.399	1.401	1.383	1.383
C^6C^7	1.397	1.411	1.413	1.394	1.395
C^5C^6	1.380	1.396	1.398	1.380	1.380
$C^{10}C^5$	1.405	1.414	1.416	1.396	1.397

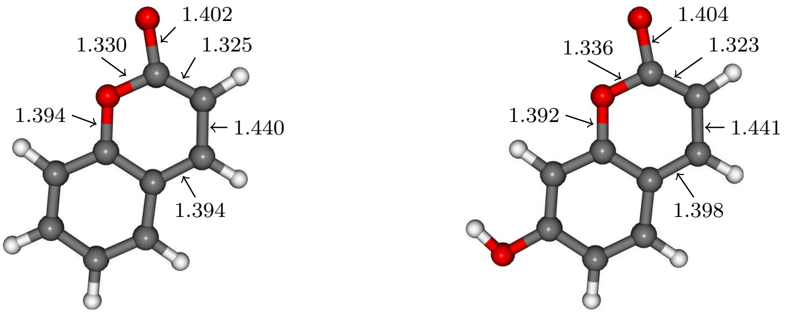

(a) Coumarin (**1**) (b) umbelliferone (**2**)

Fig. SI. 7: $1^1A''$ ($n\pi^*$) minimum geometries of coumarin and umbelliferone. All bond lengths in Å. ADC(2)/cc-pVTZ.

2.2 PES Scans

Figures SI.8 and SI.9 show how higher excited singlet state and triplet states evolve along the PES of the bond breaking pathway in umbelliferone. In particular, it can be seen how the first excited singlet $n\pi^*$ state raises along this pathway rendering a transition less probable and supporting the assumption that the branching point between the two radiationless decay channels lies close to the Franck-Condon point. The same situation applies to coumarin, as well (not shown here).

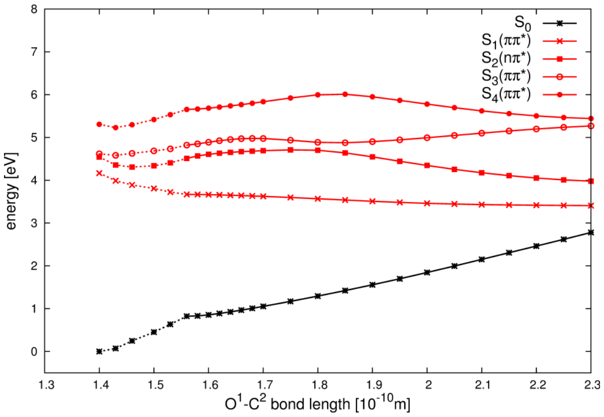

Fig. SI. 8: Relaxed PES scan along the bond breaking path in umbelliferone in the gas phase. Red curves: Excited singlet states. Black curve: Ground state. Dotted lines obtained by linear interpolation. For structure optimization cc-pVDZ and for vertical excitation energies aug-cc-pVDZ were taken as basis sets. Character of the states ($n\pi^*$ or $\pi\pi^*$) with respect to Franck-Condon point (along the reaction pathway the states start to mix and intersections occur).

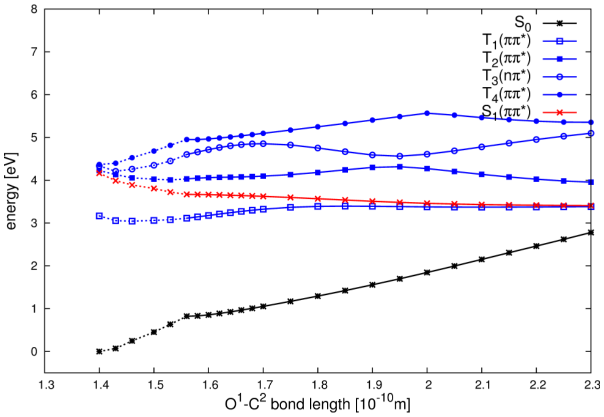

Fig. SI. 9: Relaxed PES scan along the bond breaking path in umbelliferone in the gas phase. Red curves: Excited singlet states. Blue curves: Excited triplet states. Black curve: Ground state. Dotted lines obtained by linear interpolation. For structure optimization cc-pVDZ and for vertical excitation energies aug-cc-pVDZ were taken as basis sets. Character of the states ($n\pi^*$ or $\pi\pi^*$) with respect to Franck-Condon point (along the reaction pathway the states start to mix and intersections occur).

2.3 Results for the Deprotonated, Anionic Form of Umeblliferone

Figure SI.10 shows the optimized structures for the anionic form of umbelliferone in the ground and first excited state. This molecule was only considered with inclusion of four methanol molecules as strong solvent effects can be expected and methanol is the only solvent used in this study in which it might be of importance (compare section 5.5 in the paper). The vertical excitation energies and strengths at the ground state minimum are given in Table SI.2 and the predicted fluorescence energy in Figure SI.10. Figure SI.11 shows the most important molecular orbitals for the first three excited states.

Both the predicted absorption and fluorescence energy are similar to values obtained for other umeblliferone derivatives [4, 1]. The minimum structure of the first excited state has a O^1C^2 bond length that is about 0.4 Å smaller than the one in umbelliferone itself (compare Figure 9) indicating an even larger reaction barrier for the ring opening. In order to estimate this barrier, a rough relaxed PES scan was performed starting from the excited state minimum. The result is shown in Figure 13. The barrier is much larger than in umbelliferone and an efficient suppression of this radiationless decay channel can be expected. Due to the single-reference character of the ground state wave function used in our calculations we refrain from determining an explicit value for the activation energy.

Figure 12 shows the PES along the elongation of the $O^{12}C^7$ bond (former hydroxy group) as well as the carbonyl stretching mode. The shorter bond lengths, which the original carbonyl bond (C^1O^{11}) of umbelliferone has in the ground and excited state minima, indicate a higher carbonyl character in the C^1O^{11} bond than in the deprotonated hydroxy group. At the same time, the first $n\pi^*$ transition corresponds to an excitation of a non-bonding electron from the deprotonated hydroxy group. Therefore, we have chosen to perform scans along both bonds. However, no normal mode could be clearly attributed to the stretching of the $O^{12}C^7$ bond and this bond was manually distorted to obtain the respective PES. Along both pathways none of the higher states is significantly lowered in energy in order to allow for an interaction with the first excited state and the transition into a dark $n\pi^*$ state is not observable here.

Table SI. 2: Vertical excitation energies (ΔE) and oscillator strengths (f) of the three lowest electronically excited states in the deprotonated umbelliferone with inclusion of four methanol molecules. Method: MP2/cc-pVTZ//COSMO-ADC(2)/aug-cc-pVDZ.

State	ΔE (eV)	ΔE (nm)	f	dominant contribution
2^1A ($\pi\pi^*$)	3.32	374	0.48	HOMO→LUMO (57%)
3^1A ($\pi\pi^*$)	4.34	285	0.03	HOMO→LUMO+1 (22%)/HOMO-1→LUMO(18%)
4^1A ($n\pi^*$)	4.40	282	0.00	n-HOMO→LUMO (53%)

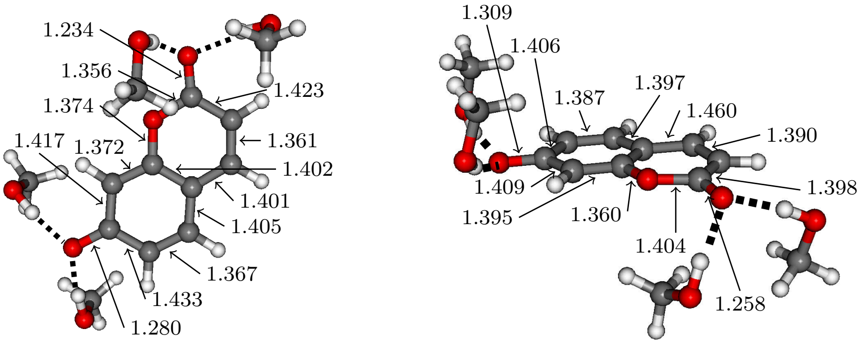

$\Delta E^{fluor} = 2.85,\ f = 0.42$

Fig. SI. 10: Optimized structures of the deprotonated umbelliferone molecule with inclusion of four methanol molecules at MP2/cc-pVTZ (ground state structure, left column) or ADC(2)/cc-pVTZ level (S_1 minimum structure, right column). All bond lengths in Å. Predicted fluorescence energy in eV (ADC(2)/aug-cc-pVTZ, with COSMO) and oscillator strength (length gauge) are given below the corresponding structure.

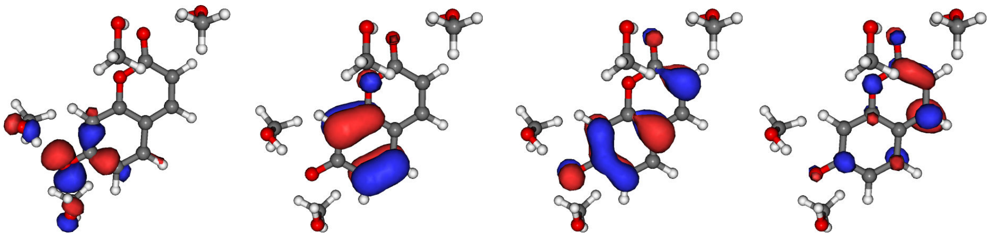

(a) n-HOMO (-12.53) (b) HOMO-1 (-9.21) (c) HOMO (-7.41) (d) LUMO (1.90)

Fig. SI. 11: Most relevant molecular orbitals (HF/aug-cc-pVDZ) of the deprotonated form of umbelliferone and their energies in eV. LUMO is the lowest unoccupied orbital when Rydberg orbitals are disregarded. n-HOMO denotes the highest occupied non-bonding orbital.

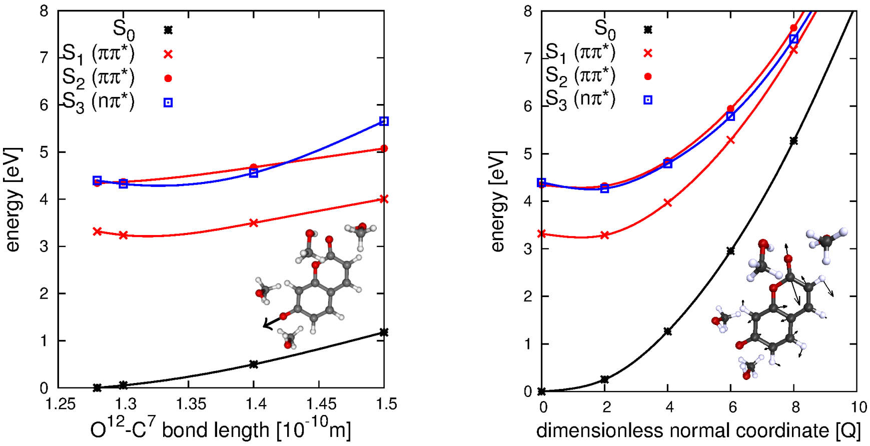

(a) (b)

Fig. SI. 12: (a) PES along the elongation of the $O^{12}C^{7}$ bond (former hydroxy group) obtained by ADC(2)/aug-cc-pVDZ+COSMO. (b) PES of the lowest excited singlet states along the carbonyl stretching mode of the deprotonated umbelliferone molecule. Frequency of the respective mode: $1737\,\mathrm{cm}^{-1}$. Distortion of 2Q leads to an elongation of the carbonyl double bond by about 0.08 Å. Structure and frequency obtained with MP2/cc-pVTZ and single point calculations with ADC(2)/aug-cc-pVDZ+COSMO.

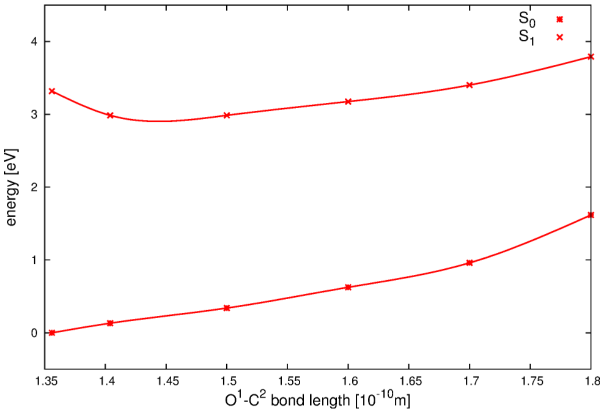

Fig. SI. 13: Relaxed PES scan along the bond breaking path in deprotonated umbelliferone with inclusion of four methanol molecules. For structure optimization cc-pVDZ and for vertical excitation energies aug-cc-pVDZ (with COSMO) were taken as basis sets. First point corresponds to the Franck-Condon point and the second one is the minimum of the S1 state as obtained by ADC(2)/cc-pVTZ (without COSMO).

2.4 Results for the Tautomerized Form of Umeblliferone

Figure SI.14 shows the optimized structures for the tautomerized form of umbelliferone in the ground and first excited state. As in the case of the anionic system, no pure gas phase calculations were made. The obtained bond lengths clearly display that the C^7O^{12} bond of the former hydroxy group has double bond character. In the ground state, the tautomerized form is about 0.9eV less stable than the original one. In the excited state, however, the energetic order is reversed and the tautomerized form is approx. 0.5 eV more stable (MP2/cc-pVTZ). The same result was obtained by Georgieva et al. [5, 6] who examined the tautomerization process along a chain of water molecules. They determined the excited state reaction barrier for such a tautomerization around 17.7 kcal/mol (0.8 eV) [6]. As methanol is slightly less basic than water this value can be seen as a lower bound for the activation barrier in methanol solution.

The vertical excitation energies and strengths at the ground state minimum are given in Table SI.3 and the predicted fluorescence energy in Figure SI.14. Figure SI.15 shows the most important molecular orbitals for the first three excited states. Again, the predicted absorption and fluorescence energies, are similar to values obtained for other umbelliferone derivatives [4, 1].

In the minimum structure of the first excited state the O^1C^2 bond length is hardly elongated in this molecule. This indicates that the ring opening pathway is even less favored due to the substantial change in the electronic structure of the molecule. Concerning the relaxation via the carbonyl stretching mode (of the former hydroxy group) no normal mode could be identified that is largely decoupled from other bond and angle deformations. Therefore, the $O^{12}C^7$ bond was again manually distorted to obtain the respective PES (Figure 16). As was already the case for the anionic form of umbelliferone no efficient transition into the dark $n\pi^*$ state seems to be possible along this pathway.

Table SI. 3: Vertical excitation energies (ΔE) and oscillator strengths (f) of the three lowest electronically excited states in the tautomerized umbelliferone with inclusion of four methanol molecules. Method: MP2/cc-pVTZ//COSMO-ADC(2)/aug-cc-pVDZ.

State	ΔE (eV)	ΔE (nm)	f	dominant contribution
2^1A ($\pi\pi^*$)	3.02	410	0.50	HOMO→LUMO (86%)
3^1A ($n\pi^*$)	3.76	330	0.00	n-HOMO→LUMO (80%)
4^1A ($\pi\pi^*$)	4.40	282	0.03	HOMO-1→LUMO (73%)

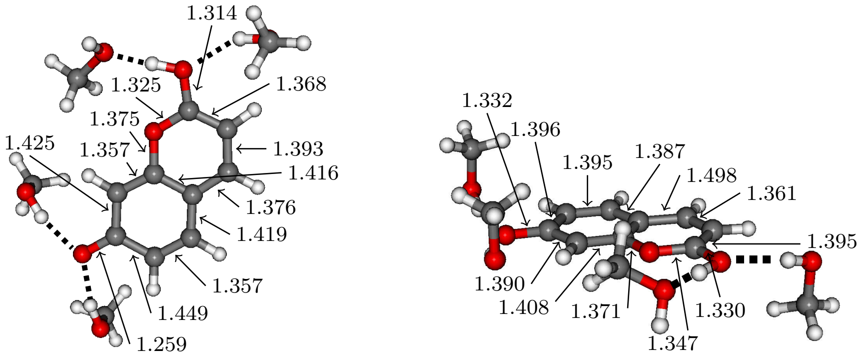

$\Delta E^{fluor} = 2.29,\ f = 0.24$

Fig. SI. 14: Optimized structures of the tautomerized umbelliferone molecule with inclusion of four methanol molecules at MP2/cc-pVTZ (ground state structure, left column) or ADC(2)/cc-pVTZ level (S_1 minimum structure, right column). All bond lengths in Å. Predicted fluorescence energy in eV (ADC(2)/aug-cc-pVTZ, with COSMO) and oscillator strength (length gauge) are given below the corresponding structure.

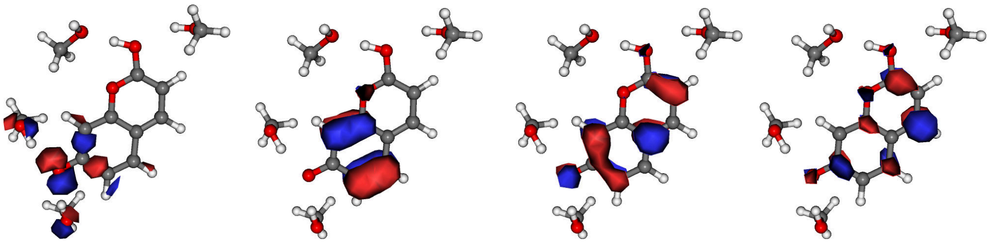

(a) n-HOMO (-11.38) (b) HOMO-1 (-9.81) (c) HOMO (-7.94) (d) LUMO (1.09)

Fig. SI. 15: Most relevant molecular orbitals (HF/aug-cc-pVDZ) of the tautomerized form of umbelliferone and their energies in eV. LUMO is the lowest unoccupied orbital when Rydberg orbitals are disregarded. n-HOMO denotes the highest occupied non-bonding orbital.

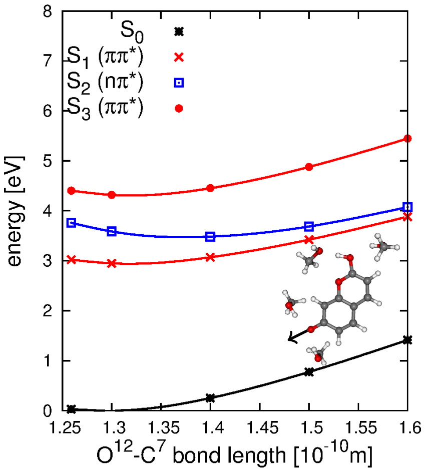

Fig. SI. 16: PES along the elongation of the $O^{12}C^{7}$ bond (former hydroxy group) obtained by ADC(2)/aug-cc-pVDZ+COSMO.

3 Coordinates of optimized structures

Calculates geometries for all stationary points given in the paper.

3.1 Coumarin

Table SI. 4: ground state, MP2/cc-pVDZ

atom	x [Å]	y [Å]	z [Å]
C	0.0568753	0.6156430	0.0000000
C	-0.2100211	-0.7708199	0.0000000
C	0.8368716	-1.7068187	0.0000000
C	2.1608793	-1.2558681	0.0000000
C	2.4467806	0.1256307	0.0000000
C	1.4016321	1.0518185	0.0000000
O	-1.4844545	-1.2702117	0.0000000
H	0.5888674	-2.7711829	0.0000000
H	2.9770609	-1.9840019	0.0000000
H	3.4843520	0.4702283	0.0000000
H	1.6076677	2.1270649	0.0000000
C	-1.0788912	1.5120432	0.0000000
C	-2.3430281	1.0074277	0.0000000
H	-0.9078756	2.5939263	0.0000000
H	-3.2288313	1.6459958	0.0000000
C	-2.6064386	-0.4372184	0.0000000

Table SI. 5: ground state, MP2/cc-pVTZ

atom	x [Å]	y [Å]	z [Å]
C	0.0567756	0.6063601	0.0000000
C	-0.2031523	-0.7630662	0.0000000
C	0.8294883	-1.6883894	0.0000000
C	2.1374010	-1.2404049	0.0000000
C	2.4183755	0.1253671	0.0000000
C	1.3841942	1.0385220	0.0000000
O	-1.4700899	-1.2512974	0.0000000
H	0.5892701	-2.7373214	0.0000000
H	2.9416345	-1.9555027	0.0000000
H	3.4387939	0.4657726	0.0000000
H	1.5857436	2.0976711	0.0000000
C	-1.0653796	1.4893885	0.0000000
C	-2.3161868	0.9972663	0.0000000
H	-0.8962800	2.5547353	0.0000000
H	-3.1835541	1.6305840	0.0000000

C	-2.5790888	-0.4285722	0.0000000

Table SI. 6: ground state, MP2/aug-cc-pVDZ

atom	x [Å]	y [Å]	z [Å]
C	0.0556064	0.6138610	0.0000000
C	-0.2053303	-0.7736765	0.0000000
C	0.8385739	-1.7129455	0.0000000
C	2.1633430	-1.2567948	0.0000000
C	2.4473722	0.1270219	0.0000000
C	1.4010738	1.0544967	0.0000000
O	-1.4883393	-1.2707764	0.0000000
H	0.5948429	-2.7773870	0.0000000
H	2.9805061	-1.9821217	0.0000000
H	3.4840011	0.4710879	0.0000000
H	1.6058368	2.1288311	0.0000000
C	-1.0780598	1.5116090	0.0000000
C	-2.3467794	1.0101658	0.0000000
H	-0.9051502	2.5919989	0.0000000
H	-3.2302016	1.6502113	0.0000000
C	-2.6081569	-0.4323485	0.0000000

Table SI. 7: ground state, MP2/aug-cc-pVTZ

atom	x [Å]	y [Å]	z [Å]
C	0.0562537	0.6069330	0.0000000
C	-0.2028796	-0.7634105	0.0000000
C	0.8288213	-1.6895375	0.0000000
C	2.1365249	-1.2402858	0.0000000
C	2.4186864	0.1256984	0.0000000
C	1.3849079	1.0395604	0.0000000
O	-1.4707960	-1.2524677	0.0000000
H	0.5892831	-2.7411496	0.0000000
H	2.9433010	-1.9568389	0.0000000
H	3.4425183	0.4644993	0.0000000
H	1.5875808	2.1008194	0.0000000
C	-1.0654816	1.4901533	0.0000000
C	-2.3168849	0.9979071	0.0000000
H	-0.8968132	2.5578436	0.0000000
H	-3.1888444	1.6301101	0.0000000
C	-2.5777524	-0.4286493	0.0000000

Table SI. 8: $2^1A'$, ADC(2)/aug-cc-pVTZ

atom	x [Å]	y [Å]	z [Å]
C	0.461301	0.801650	0.161073
C	0.360498	-0.604125	0.314005
C	1.453450	-1.428956	0.106600
C	2.707980	-0.889439	-0.238532
C	2.808658	0.463864	-0.375035
C	1.676726	1.311323	-0.190227
O	-0.783392	-1.143946	0.726326
H	1.315107	-2.490454	0.248087
H	3.560072	-1.534185	-0.382398
H	3.756744	0.915931	-0.624673
H	1.792648	2.377325	-0.322712
C	-0.713624	1.657919	0.344744
C	-1.991393	1.224034	0.043711
H	-0.554536	2.693667	0.602524
H	-2.816284	1.923072	0.042020
C	-2.365087	-0.067999	-0.190330

Table SI. 9: $2^1A'$, TD-B3LYP/aug-cc-pVTZ

atom	x [Å]	y [Å]	z [Å]
C	0.0509399	0.6342537	0.1027778
C	-0.1816931	-0.7771335	0.2423900
C	0.8685121	-1.7108389	0.0142286
C	2.1651454	-1.2746460	-0.2388503
C	2.4055030	0.0883194	-0.3108911
C	1.3427033	1.0275982	-0.1534944
O	-1.3317480	-1.2232448	0.6571853
H	0.6254604	-2.7608129	0.1008964
H	2.9668128	-1.9856274	-0.3754806
H	3.4043559	0.4576381	-0.4972588
H	1.5694575	2.0829671	-0.2388247
C	-1.0802350	1.5287062	0.1942587
C	-2.3729810	1.0262329	0.1188052
H	-0.9125627	2.5946514	0.1806573
H	-3.2237098	1.6867349	0.0218186
C	-2.6946556	-0.3279959	0.1899808

Table SI. 10: $2^1A'$, TD-BHLYP/aug-cc-pVTZ

atom	x [Å]	y [Å]	z [Å]

C	0.0422467	0.6574864	-0.0061200
C	-0.2096834	-0.7751945	-0.0003099
C	0.8360214	-1.7009317	0.0067199
C	2.1359971	-1.2669628	0.0040776
C	2.3989374	0.1174228	-0.0046038
C	1.3837595	1.0480204	-0.0094842
O	-1.4310743	-1.2508939	-0.0049643
H	0.5816904	-2.7433383	0.0120521
H	2.9464974	-1.9685312	0.0080263
H	3.4185255	0.4542080	-0.0070317
H	1.6175985	2.0956867	-0.0152304
C	-1.0536517	1.5172635	-0.0058805
C	-2.3454199	0.9951086	0.0039495
H	-0.8953753	2.5778550	-0.0096844
H	-3.2124734	1.6233565	0.0084933
C	-2.5930165	-0.3877351	0.0058146

Table SI. 11: $1^1A''$, ADC(2)/cc-pVTZ

atom	x [Å]	y [Å]	z [Å]
C	0.0458470	0.6480527	0.0000000
C	-0.1937333	-0.7392974	0.0000000
C	0.8143074	-1.6797256	0.0000000
C	2.1334404	-1.2568661	0.0000000
C	2.4150099	0.1114716	0.0000000
C	1.4010550	1.0420695	0.0000000
O	-1.4954545	-1.2375128	0.0000000
H	0.5541780	-2.7248149	0.0000000
H	2.9298267	-1.9800904	0.0000000
H	3.4390062	0.4445138	0.0000000
H	1.6257156	2.0967251	0.0000000
C	-1.0344433	1.5293289	0.0000000
C	-2.3653062	0.9804293	0.0000000
H	-0.8825746	2.5955242	0.0000000
H	-3.2450923	1.5961878	0.0000000
C	-2.4769449	-0.3402802	0.0000000

Table SI. 12: ground state + 2 MeOH, MP2/cc-pVTZ

atom	x [Å]	y [Å]	z [Å]
O	0.3427540	0.6014098	0.9682599
C	-0.7433006	-0.2165405	0.8808565

C	-0.5669057	-1.4890836	0.2253242
C	0.6221806	-1.8363523	-0.3036073
C	2.9955872	-1.2311904	-0.7585590
C	4.0230390	-0.3189871	-0.6415308
C	3.8079983	0.8935783	0.0144427
C	2.5695932	1.1918593	0.5508310
C	1.5452705	0.2672978	0.4258026
C	1.7356355	-0.9499736	-0.2247836
O	-1.7876363	0.1908551	1.3571286
H	2.3796083	2.1192578	1.0626186
H	4.9904824	-0.5417568	-1.0555565
H	3.1485108	-2.1715465	-1.2628542
H	0.7400157	-2.7872113	-0.7989654
H	-1.4406460	-2.1142757	0.1765582
H	-3.2578466	-0.9474235	0.7934433
O	-3.7373607	-1.5391820	0.2004323
C	-3.8081985	-0.8741750	-1.0470127
H	-4.1371020	0.1561208	-0.9461151
H	-4.5190119	-1.4120135	-1.6624236
H	-2.8463308	-0.8734677	-1.5634074
H	-2.3263717	1.8642038	0.4236394
O	-2.5046310	2.4091881	-0.3509633
C	-1.4295894	2.2267359	-1.2436192
H	-1.2978351	1.1813029	-1.5278156
H	-0.4872206	2.5942565	-0.8397081
H	-1.6574910	2.7880560	-2.1418331

Table SI. 13: $2^1A'$ + 2 MeOH, ADC(2)/cc-pVTZ

atom	x [Å]	y [Å]	z [Å]
O	0.7761383	-1.2758436	1.4827962
C	-1.1560412	-0.9216446	0.6721394
C	-0.9955066	-1.3407567	-0.6272148
C	0.2045222	-1.4214411	-1.2826352
C	2.3027436	-0.1326648	-1.5654077
C	3.4208851	0.5572873	-1.0252010
C	3.6144757	0.6538807	0.3258011
C	2.6839837	0.0342110	1.1723501
C	1.5995103	-0.6568503	0.6491757
C	1.3946901	-0.7443416	-0.7520554
O	-1.6263172	-0.2363718	1.5219236
H	2.7890964	0.0594091	2.2441980
H	4.1235160	1.0086184	-1.7051293
H	2.1774838	-0.1736340	-2.6351766

H	0.2512841	-1.8647963	-2.2627440
H	-1.9148563	-1.6846363	-1.0767598
H	-4.0490018	-0.6457939	0.6331725
O	-4.0924160	-0.7223680	-0.3223195
C	-4.0433808	0.5905811	-0.8579146
H	-3.2013966	1.1641463	-0.4795563
H	-4.9594673	1.1416249	-0.6574329
H	-3.9383461	0.4866554	-1.9306354
H	-1.4734370	1.7363274	1.0546784
O	-1.3080404	2.5281526	0.5341503
C	-0.2327459	2.2393642	-0.3376718
H	-0.4904165	1.4725360	-1.0669661
H	0.6588092	1.9181170	0.2000021
H	0.0029648	3.1543233	-0.8678880

3.2 Umbelliferone

Table SI. 14: ground state, MP2/cc-pVTZ

atom	x [Å]	y [Å]	z [Å]
C	-0.0187094	1.0303341	-0.0000026
C	-0.0210558	-0.3620914	-0.0000038
C	1.1591115	-1.0866982	-0.0000025
C	2.3655140	-0.4105503	0.0000000
C	2.3946933	0.9838605	0.0000015
C	1.2130619	1.6882126	0.0000000
O	-1.1745371	-1.0759910	-0.0000033
H	1.1133909	-2.1630219	-0.0000015
O	3.5624784	-1.0503778	0.0000034
H	3.3469294	1.4828432	0.0000046
H	1.2280836	2.7660522	0.0000017
C	-1.2816048	1.6904151	-0.0000004
C	-2.4227208	0.9780448	0.0000015
H	-1.3108359	2.7687471	0.0000011
H	-3.3909609	1.4422243	0.0000047
C	-2.4195898	-0.4695476	0.0000006
O	-3.3917374	-1.1788115	0.0000037

Table SI. 15: $2^1A'$, ADC(2)/aug-cc-pVTZ

atom	x [Å]	y [Å]	z [Å]
C	-0.1509927	0.9664872	0.2259884
C	0.0399409	-0.4050997	0.5327613

C	1.2857688	-1.0066765	0.3472959
C	2.3756252	-0.2679892	-0.1159362
C	2.1868236	1.0504213	-0.4312904
C	0.9134569	1.6540251	-0.2795663
O	-0.9537936	-1.1284447	0.9993759
H	1.3758381	-2.0530542	0.6035370
O	3.6181740	-0.8055186	-0.2855403
H	3.0204257	1.6309131	-0.7954518
H	0.7984311	2.6915348	-0.5567003
C	-1.4780877	1.5780555	0.4060722
C	-2.6177273	0.9049567	-0.0029405
H	-1.5606076	2.5508224	0.8648204
H	-3.5926834	1.3680511	0.0507641
C	-2.6464891	-0.4000505	-0.3769310
O	-2.8250683	-1.4054882	-0.9525161

Table SI. 16: 1^1A“, ADC(2)/cc-pVTZ

atom	x [Å]	y [Å]	z [Å]
C	-0.1273142	0.8265003	0.0000000
C	-0.3677639	-0.5556093	0.0000000
C	0.6378063	-1.5018328	0.0000000
C	1.9552903	-1.0821331	0.0000000
C	2.2443257	0.2820188	0.0000000
C	1.2295666	1.2090922	0.0000000
O	-1.6649239	-1.0606309	0.0000000
H	0.3751765	-2.5474249	0.0000000
O	3.0108510	-1.9463832	0.0000000
H	3.2752798	0.5901494	0.0000000
H	1.4643301	2.2612806	0.0000000
C	-1.2061405	1.7150585	0.0000000
C	-2.5357890	1.1607016	0.0000000
H	-1.0532900	2.7806701	0.0000000
H	-3.4172694	1.7744259	0.0000000
C	-2.6490070	-0.1576810	0.0000000
O	-3.8375737	-0.9042646	0.0000000

Table SI. 17: ground state + 2MeOH, MP2/cc-pVTZ

atom	x [Å]	y [Å]	z [Å]
H	-1.9711116	4.4604803	0.5233611
O	-1.1507283	4.6524194	0.0587473
C	-0.4111368	3.5196579	-0.0106822

C	-0.8329575	2.3164461	0.5249522
C	-0.0121442	1.2086337	0.4065584
O	-0.4713865	0.0502316	0.9502580
C	1.2220169	1.2705106	-0.2336184
C	1.6234988	2.4997243	-0.7647465
C	0.8226710	3.6115963	-0.6583046
H	1.1230043	4.5606243	-1.0645129
H	2.5763841	2.5660370	-1.2639140
H	-1.7791886	2.2198792	1.0307919
C	1.9890950	0.0751733	-0.3024176
C	1.5194255	-1.0730605	0.2259551
C	0.2327823	-1.1171003	0.8695162
O	-0.2894816	-2.1102616	1.3445354
H	2.0547412	-2.0045827	0.1836791
H	2.9511986	0.0944935	-0.7897365
H	0.7079369	-3.6879967	0.8189325
O	1.2350929	-4.2453158	0.2329556
C	0.5653634	-4.2468842	-1.0138130
H	0.6844170	-3.2985423	-1.5411922
H	-0.4977964	-4.4445398	-0.9098596
H	1.0097710	-5.0259772	-1.6211237
H	-1.9946765	-2.4528539	0.4067149
O	-2.5735045	-2.5621857	-0.3565409
C	-2.2502769	-1.5412195	-1.2720044
H	-2.8381895	-1.7107548	-2.1661949
H	-1.1970716	-1.5559125	-1.5570123

Table SI. 18: ground state + 4MeOH, MP2/cc-pVTZ

atom	x [Å]	y [Å]	z [Å]
H	-1.4220743	3.3590647	-0.7386992
O	-0.4995158	3.4000127	-1.0701423
C	0.1379250	2.2420200	-0.7778156
C	-0.5223350	1.1586085	-0.2215398
C	0.1990916	0.0097757	0.0483702
O	-0.4912211	-1.0265892	0.5978150
C	1.5609363	-0.0916106	-0.2234476
C	2.2004874	1.0177472	-0.7848848
C	1.5053379	2.1715650	-1.0601163
H	1.9937613	3.0353455	-1.4753488
H	3.2551611	0.9587390	-0.9996882
H	-1.5766178	1.1950391	-0.0092450
C	2.2052621	-1.3196787	0.0874607
C	1.5089699	-2.3466423	0.6167162

C	0.0996079	-2.2236766	0.8787436
O	-0.6189410	-3.1020742	1.3250861
H	1.9486863	-3.2997211	0.8491304
H	3.2599796	-1.4258215	-0.1126354
H	0.3032395	-4.7982452	1.2560410
O	0.8966180	-5.4693659	0.8960824
C	0.5770075	-5.5761870	-0.4781211
H	0.9400704	-4.7191450	-1.0486189
H	-0.4928457	-5.6651963	-0.6459283
H	1.0670853	-6.4640480	-0.8589661
H	-2.0735885	-3.4208168	0.0262144
O	-2.4647549	-3.6043997	-0.8358276
C	-1.8231255	-2.7678350	-1.7711003
H	-2.1938231	-3.0375015	-2.7529314
H	-0.7402825	-2.9015299	-1.7745122
H	-2.0374724	-1.7133772	-1.6015476
O	-2.8679428	3.3030895	0.1734787
H	-3.6916729	3.6966653	-0.1224926
C	-2.5903329	3.7518977	1.5010999
H	-2.4680805	4.8295148	1.5390959
H	-3.3721580	3.4444443	2.1867812
H	-1.6610022	3.2809698	1.7940836
H	0.6729019	4.8741204	-0.6380359
O	1.3953864	5.3729106	-0.2400841
C	1.4562545	4.9803707	1.1135618
H	2.2943591	5.4973156	1.5648513
H	0.5570024	5.2537439	1.6654466

Table SI. 19: $2^1A'$ + 2 MeOH, ADC(2)/cc-pVTZ

atom	x [Å]	y [Å]	z [Å]
H	-2.297382	4.171552	1.437101
O	-1.699830	4.502292	0.747357
C	-0.791410	3.533663	0.473998
C	-0.748658	2.296954	1.117745
C	0.258635	1.374551	0.786312
O	0.336691	0.267030	1.535584
C	1.217522	1.648633	-0.280739
C	1.140805	2.927285	-0.908206
C	0.166100	3.847964	-0.541702
H	0.104648	4.830361	-1.017593
H	1.856604	3.167493	-1.699603
H	-1.444165	2.035373	1.921425
C	2.140331	0.637221	-0.633571

C	1.867764	-0.700967	-0.118014
C	1.009253	-0.902616	0.941943
O	0.643658	-1.959516	1.541160
H	2.332324	-1.593925	-0.544225
H	2.875602	0.799042	-1.426324
H	1.306438	-3.387368	0.398337
O	1.530774	-3.853730	-0.423555
C	0.385658	-3.701787	-1.250607
H	0.381311	-2.726074	-1.776820
H	-0.556610	-3.781116	-0.683470
H	0.409015	-4.494831	-2.013613
H	-1.203267	-2.381025	1.366356
O	-2.064324	-2.465914	0.921469
C	-2.238556	-1.269233	0.192819
H	-3.165415	-1.368863	-0.392480
H	-1.410597	-1.072327	-0.516552

Table SI. 20: $2^1A'$ + 4 MeOH, ADC(2)/cc-pVTZ

atom	x [Å]	y [Å]	z [Å]
H	-1.4600694	3.2008633	-0.5461776
O	-0.4964244	3.2991026	-0.7363516
C	0.1500567	2.1615490	-0.4294199
C	-0.4935559	1.0422150	0.0634522
C	0.2445046	-0.0848979	0.3756176
O	-0.4184564	-1.0954640	0.9396218
C	1.6704139	-0.1409959	0.1530556
C	2.2846595	1.0227944	-0.3463794
C	1.5530145	2.1524277	-0.6272592
H	2.0198319	3.0493399	-0.9986706
H	3.3486800	1.0129778	-0.5140082
H	-1.5574746	1.0336913	0.2227394
C	2.3454254	-1.3368367	0.4151083
C	1.5435169	-2.4909382	0.7105139
C	0.2008594	-2.3949117	0.9670303
O	-0.6466179	-3.2868977	1.2244862
H	1.9622892	-3.4812852	0.7278660
H	3.4091463	-1.4155838	0.2726629
H	0.1890330	-4.9437490	0.7949679
O	0.7233890	-5.6013290	0.3286221
C	0.4536450	-5.4131040	-1.0462665
H	0.9232268	-4.5067907	-1.4326585
H	-0.6125322	-5.3559601	-1.2516725
H	0.8670221	-6.2606656	-1.5805462

H	-1.9923073	-3.1650293	-0.0990752
O	-2.3857088	-3.1256345	-0.9828615
C	-1.6009258	-2.2400173	-1.7465653
H	-1.8934172	-2.3558643	-2.7845030
H	-0.5353388	-2.4595291	-1.6702108
H	-1.7545914	-1.1978063	-1.4634311
O	-3.0246575	3.0029550	-0.0080490
H	-3.8107894	3.1852033	-0.5273880
C	-3.2507420	3.3987884	1.3461201
H	-3.4442276	4.4635660	1.4203366
H	-4.0734711	2.8416133	1.7796928
H	-2.3439018	3.1643689	1.8877556
H	0.6906437	4.8774950	-0.9692776
O	1.4982611	5.3814678	-0.8264579
C	1.6433963	5.5194283	0.5726262
H	2.5574396	6.0722678	0.7489643
H	0.8192535	6.0721609	1.0195169

References

[1] T. Moriya, *Bull. Chem. Soc. Jpn.* **61**, 1873 (1988).

[2] E. Bardez, P. Boutin, and B. Valeur, *Chem. Phys. Lett.* **191**, 142 (1992).

[3] T.-J. Hsieh, C.-C. Su, C.-Y. Chen, C.-H. Liou, and L.-H. Lu, *J. Mol. Struct.* **741**, 193 (2005).

[4] J. S. Seixas de Melo, C. Cabral, J. C. Lima, and A. L. Maçanita, *J. Phys. Chem. A* **115**, 8392 (2011).

[5] I. Georgieva, N. Trendafilova, A. Aquino, and H. Lischka, *J. Phys. Chem. A* **109**, 11860 (2005).

[6] I. Georgieva, N. Trendafilova, A. J. A. Aquino, and H. Lischka, *J. Phys. Chem. A* **111**, 127 (2007).